



## Synthesis of porous hydroxyapatite scaffolds from waste cockle shells by polyurethane sponge replication method

**Fitri Afriani<sup>1\*</sup>, Anisa Indriawati<sup>1</sup>, Widodo Budi Kurniawan<sup>1</sup>, Yekti Widyaningrum<sup>1</sup>,  
Rifqi Almusawi Rafsanjani<sup>2</sup>, Yuant Tiandho<sup>1</sup>**

<sup>1</sup>*Department of Physics, University of Bangka Belitung, Indonesia*

<sup>2</sup>*Department of Physics, University of Indonesia, Indonesia*

\*E-mail: fitriiafriani@gmail.com

(Received: 28 November 2019; Revised: 28 January 2020; Accepted: 29 February 2020)

### ABSTRACT

Researchers have synthesized hydroxyapatite-based porous scaffolds by the polyurethane sponge replication methods. Hydroxyapatite was derived from waste cockle shells through the co-precipitation method. The synthesis of porous scaffolds through the sponge replication methods is carried out by absorbing hydroxyapatite slurry through the addition of PVA and then followed by heating at 900°C to decompose the polyurethane and PVA. The best of slurry that can produce a porous scaffold in this study is the slurry that prepared through the ratio of hydroxyapatite:PVA = 80:20. The decomposition of the two polymers will leave macropores on the scaffold with an average size of 460 µm. Based on the thermogravimetric analysis, X-ray diffraction and FTIR spectrophotometer revealed that the PVA and polyurethane sponge were correctly decomposed, except for scaffolds with 40% PVA. Thus, the porous scaffolds synthesized in this study satisfies the requirements of porous scaffolds for the bone therapy process.

**Keywords:** a biocompatible material, hydroxyapatite, scaffold

DOI: [10.30870/gravity.v6i1.6741](https://doi.org/10.30870/gravity.v6i1.6741)

### INTRODUCTION

The use of scaffolds is a promising alternative solution in the process of bone therapy. Through these methods, problems that often arise in conventional bone therapy methods such as scarcity of donors, infections, and potential trauma can be overcome (Huang, 2018). One biocompatible material that is widely used in the synthesis of bone scaffolds is hydroxyapatite ( $\text{Ca}_5(\text{PO}_4)_3(\text{OH})$ ) (Esposti et al., 2019). The chemical and physical composition of hydroxyapatite also resembles human bone mineral constituent. To improve the bio-

compatibility of hydroxyapatite when interacting with bone cells, in recent years, have been developed synthesize methods for hydroxyapatite based on natural materials such as egg-shells (Nunez et al., 2018) and animal bones (Gunawan et al., 2019). As a maritime nation, one of the impressive natural materials to be developed into hydroxyapatite in Indonesia is waste cockle shells. The main composition of cockle shells is aragonite. Through calcination, it can be decomposed into CaO and can be used as raw material for hydroxyapatite (Afriani et al., 2018; Afriani et al., 2019).

Along with the development of the bone scaffold research, nowadays, there are several requirements for scaffolds to be used in bone therapy. Some of these requirements include: (a) biocompatible, (b) material can induce bonding bones, (c) the level of biodegradability that corresponds to the growth and formation of bone tissue, (d) the mechanical strength of the scaffold can prop up load before the regeneration of new bone tissue and (e) the porous of structures are more than 100  $\mu\text{m}$  to cell penetration, tissue growth, and vascularization can work well (Han et al., 2010). Therefore, the development of hydroxyapatite based scaffolds has focused on the development of porous scaffolds.

Several methods can be used to produce a porous scaffold such as porogen replication (Zhang et al., 2019), foaming (Meskinfam et al., 2018), and freeze-drying (Afriani et al., 2015). Each of these methods can produce different pore morphology. Porogen replication method can provide a homogeneous pore and has a good interconnection. Also, through this method, the shape of pore size can be easily controlled. One of the porogen material that can be utilized in the replication method is polyurethane (PU) sponge. PU is a polymer that is easily decomposed through thermal treatment, easy to obtain, and cheap (Li et al., 2015). Therefore, based on these aspects, in this paper will be presented study related to the synthesis of porous hydroxyapatite scaffold from waste cockle shells using the PU sponge replication method with the addition of polyvinyl alcohol (PVA) as a slurry medium. PVA is used because it is a biocompatible material and it has been widely used in tissue engineering (Waluyo & Sabarman, 2019; Chahal et al., 2013).

## RESEARCH METHODS

This research is an experimental research and conducted at the Laboratory of Physics - University of Bangka Belitung, Physics Research Centre - Indonesian Institute of Sciences, and the Lab. UPP-IPD Natural Sciences - University of Indonesia. The equipment used in this study includes magnetic stirrer, furnace,

thermogravimetric analysis (TGA), x-ray diffraction (XRD), and Fourier transform infrared spectrophotometer (FTIR). Materials used include waste cockle shells from Pangkalpinang areas,  $(\text{NH}_4)_2\text{HPO}_4$ , polyurethane sponge (PU), and polyvinyl alcohol (PVA).

In summary, procedure of this research is divided into two stages, namely: (1) the synthesis of hydroxyapatite from waste cockle shells and (2) a porous scaffold synthesis using polymer sponge replication. Hydroxyapatite synthesis process starting from preparation of waste cockle shells consisting of cleaning subsequently mashed up and calcined at a temperature of 1000°C for 3 hours. 1000°C temperature is the calcination temperature of cockle shells that can be decomposing into calcium oxide perfectly (CaO) (Afriani et al., 2018). Hydroxyapatite powder synthesized from a mixture of calcined cockle shells powder and  $(\text{NH}_4)_2\text{HPO}_4$  with a ratio Ca/P of 1.67 through co-precipitation method. After the solution is aged for 24 hours, precipitates are filtered and calcined at temperatures of 900°C for 5 hours. Preparation of porous scaffold made by substituted hydroxyapatite slurry phase into a sponge PU. Hydroxyapatite slurry preparing by mixing hydroxyapatite with the polyvinyl alcohol (PVA) with a variation of the ratio of hydroxyapatite:PVA at 80:20 (PVA-20), 70:30 (PVA-30), and 60:40 (PVA-40). After a sponge impregnated by slurry, then it is heated at a temperature of 900°C for 2 hours to decompose sponge and PVA and create pores in the scaffolds. The TGA/DTG is used to observe the thermal characteristics of PVA and PU sponge, scaffolds crystalline phase analysis by XRD, and the functional groups in scaffolds is determined by FTIR.

## RESULTS AND DISCUSSION

XRD analysis of hydroxyapatite powder in this study is presented in Figure 1. Based on the comparison between the spectrum of hydroxyapatite powder in this study with the database can be stating that the spectrum in accordance with the standard data of hydroxyapatite: PDF2-01-084-1998. The three highest peaks associated with hydroxyapatite, among

others, lies in the  $2\theta$  angle:  $31.99^\circ$ ,  $33.09^\circ$ , and  $32.39^\circ$ .

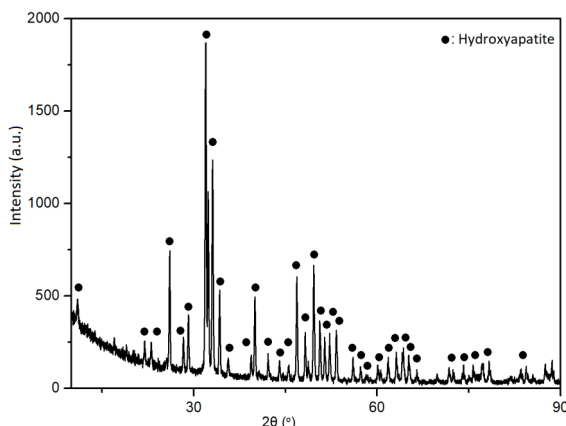


**Figure 1.** XRD pattern of hydroxyapatite

In Figure 2 are shown the results of the analysis of TGA/DTG of PVA and PU. It appears that the thermal treatment process at a temperature of  $900^\circ\text{C}$  will leave only the PU in a relatively small amount (<10%). Thus, the

scaffolds formed by a sponge replication method will be dominated by hydroxyapatite.

Through the PVA decomposition curve in Figure 2(a), it seems that the decomposition process consists of three stages. The peak of first, second, and third stage occurs at a temperature of  $106^\circ\text{C}$ ,  $326^\circ\text{C}$ , and  $402^\circ\text{C}$ , respectively. The first decomposition at a temperature of  $106^\circ\text{C}$  associated with the evaporation of water adsorbed. While decomposition on the second and third peaks related to the decomposition of the edge and the main chain of PVA, respectively (Awada & Daneault, 2015).

For the PU, appears that the mass decomposition curve consists of three stages. The culmination of the first phase occurs at a temperature of  $295^\circ\text{C}$ , the peak of the second stage occurs at  $367^\circ\text{C}$ , and the peak of the third phase occurs at a temperature of  $738^\circ\text{C}$ . The first stage of the PU decomposition process relates to the urethane decomposition, while for the second and third stages relate to

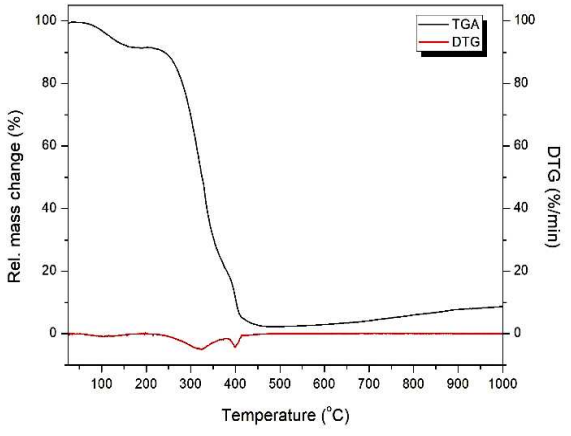


**Figure 2.** TGA and DTG patterns for: (a) PVA and (b) sponge PU

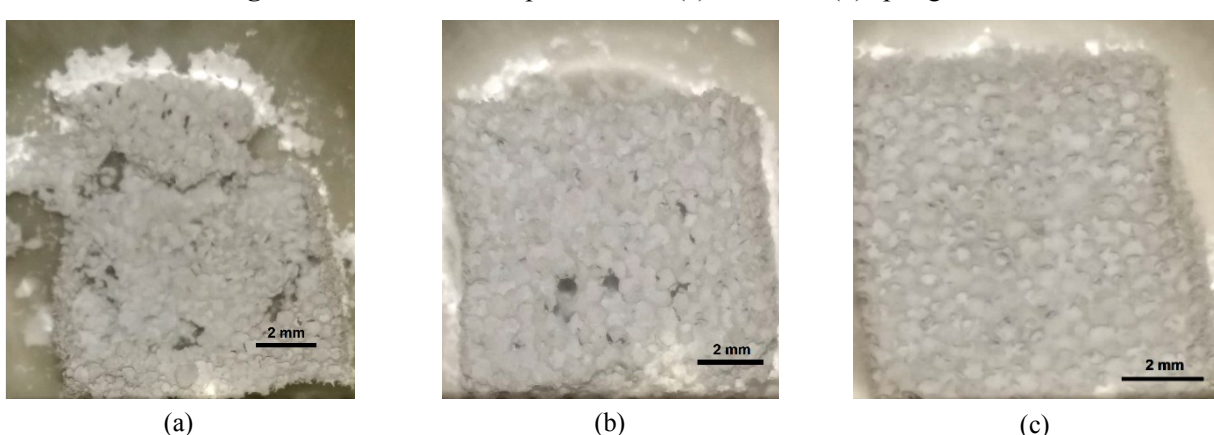
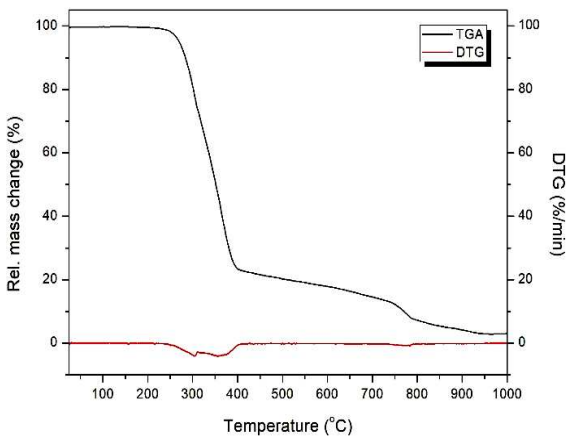


**Figure 3.** Photograph of scaffolds: (a) PVA-40; (b) PVA-30; (c) PVA-20

the ester bond (Trovati et al., 2010). The low of first decomposition temperature in this study ( $<400^{\circ}\text{C}$ ) occurred because the sponge thermal treatment process was carried out under atmospheric conditions (Mikulcic et al., 2019). After the heat treatment process, the PU will decompose to leave a relatively round pore as shown in Figure 3. It appears that the PVA-20 have a good shape. Meanwhile, PVA-30 and PVA-40 are fragile. The higher levels of PVA will reduce hydroxyapatite in a slurry. Thus, for both samples just leaving a little amount of hydroxyapatite and it was unable to support scaffolds.

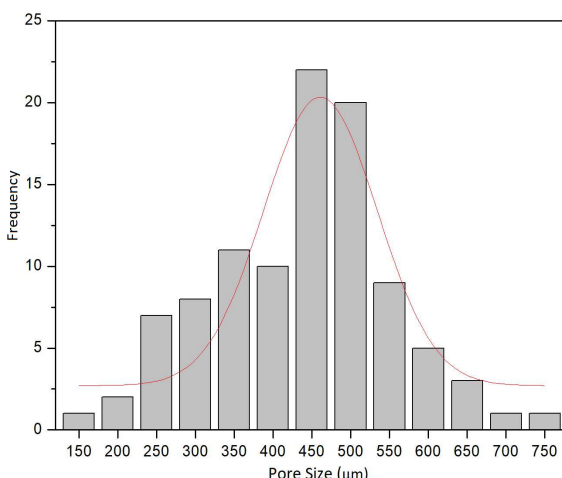


Figure 4. Pore size distribution of PVA-20

Analysis of pore size on the scaffold PVA-20 in Figure 4, shows that the average pore of the scaffold is  $460\ \mu\text{m}$ . Thus, according to pore size, it can be stated that the scaffold belongs to the macropore scaffold and it can support the growth of bone cells (Sopyan & Gunawan, 2013).

The XRD pattern of scaffolds is present in Figure 5. Through these results, it appears that almost all of the XRD peaks correspond to the hydroxyapatite peaks. These indicate that the synthesis of the porous scaffold through a sponge replication method does not produce a new crystalline phase.

Figure 6 shows the FTIR spectra of hydroxyapatite powder and scaffolds. Through the analysis of the FTIR spectra of hydroxyapatite powder is found that the specific functional group of the hydroxyapatite is asymmetric stretching vibration of P-O and it arises

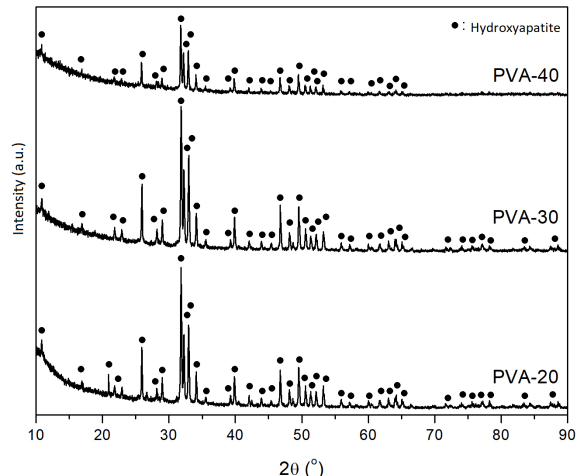


Figure 5. XRD pattern of scaffolds

from  $\text{PO}_4^{3-}$  at  $1150$  to  $1000\ \text{cm}^{-1}$ . Absorption peak associated with the symmetric stretching vibration of  $\text{PO}_4^{3-}$  occurs at  $960\ \text{cm}^{-1}$ . Absorption peak associated with the bending vibration of  $\text{PO}_4^{3-}$  occurs at  $560$ - $620\ \text{cm}^{-1}$ . Also, another absorption peak that appears at  $3573\ \text{cm}^{-1}$ ,  $630\ \text{cm}^{-1}$ , and  $471\ \text{cm}^{-1}$  indicate the presence of OH groups in hydroxyapatite powder (Azis et al., 2015). The FTIR spectra on porous scaffold PVA-20 and PVA-30 did not show any significant differences with the FTIR pattern of hydroxyapatite. These indicate that the scaffolding is not forming new functional groups. However, different things happen on the scaffold PVA-40 that has absorption peak at  $1745\ \text{cm}^{-1}$  and it corresponds to the C=O group, although at low intensity (Li et al., 2015). The emergence of the C=O group originates from the remaining PVA in the scaffold that does not completely decompose. This is the impact of PVA-40 slurry

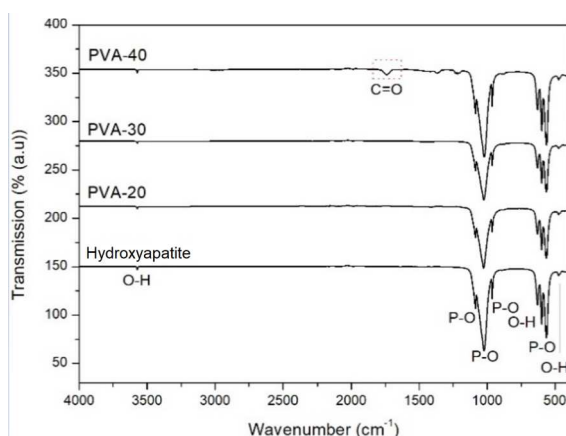


Figure 6. The FTIR patterns of hydroxyapatite powder and scaffolds

which contains PVA in a higher amount than the others.

## CONCLUSION

Based on the XRD patterns analysis has been shown that the hydroxyapatite could be synthesized from waste cockle shells through the co-precipitation method. According to the TGA/DTG analysis can seem that the heating process at 900°C quite useful to decompose PU and PVA. The best slurry that can produce a porous scaffold is the PVA-20. Measurements of micrographs showed that the porous structure of the scaffold has an average pore size of 460 µm. Based on this, it can be stated that the synthesized porous scaffold can support bone cell growth properly. Also, according to the analysis of FTIR spectra and XRD pattern showed that porous scaffolding, except for PVA-40, did not have significant amounts of PU and PVA.

## ACKNOWLEDGMENT

This research was funded by University of Bangka Belitung through scheme: Penelitian Dosen Tingkat Jurusan (PDTJ) in 2019 .

## REFERENCES

- Afriani, F., Dahlan, K., Nikmatin, S., & Zuas, O. (2015). Alginate affecting the characteristics of porous beta-TCP/alginate composite scaffolds. *Journal of Optoelectronics and Biomedical Materials*, 7(3), 67-76.
- Afriani, F., Mustari, & Tiandho, Y. (2018). Pengaruh Lama Pemanasan Terhadap Karakteristik Kristal Kalsium dari Limbah Cangkang Kerang. *Edumatsains: Jurnal Pendidikan, Matematika, dan Sains*, 2(2), 189-200.
- Afriani, F., Tiandho, Y., Evi, J., & Rafsanjani, R. (2019). Synthesis and characterization of hydroxyapatite/silica composites based on cockle shells waste and tin tailings. *IOP Conference Series: Earth and Environmental Science*, 353, 012032.
- Awada, H., & Daneault, C. (2015). Chemical modification of poly(vinyl alcohol) in water. *Applied Science*, 5, 840-850.
- Azis, Y., Jamarun, N., Zultiniar, Arief, S., & Nur, H. (2015). Synthesis of hydroxyapatite by hydrothermal method from cockle shell. *Journal of Chemical and Pharmaceutical Research*, 7(5), 798-804.
- Chahal, S., Hussain, F., & Yusoff, M. (2013). Characterization of modified cellulose (MC)/poly (vinyl alcohol) electrospun nanofibers for bone tissue engineering. *Procedia Engineering*, 53, 683-688.
- Esposti, M., Chiellini, F., Bondioli, F., Morselli, D., & Fabbri, P. (2019). Highly porous PHB-based bioactive scaffolds for bone tissue engineering by in situ synthesis of hydroxyapatite. *Materials Science & Engineering: C*, 100, 286-296.
- Gunawan, G., Arifin, A., Yani, I., & Indrajaya, M. (2019). Characterization of porous hydroxyapatite-alumina composite scaffold produced via powder compaction method. *IOP Conference Series: Materials Science and Engineering*, 620, 012107.
- Han, J., Zhou, Z., Yin, R., Yang, D., & Nie, J. (2010). Alginate-chitosan/hydroxyapatite polyelectrolyte complex porous scaffolds: Preparation and characterization. *International Journal of Biological Macromolecules*, 46, 199-205.
- Huang, C., Hao, N., Bhagia, S., Li, M., Meng, X., Pu, Y., . . . Ragauskas, A. (2018). Porous artificial bone scaffold synthesized from a facile in situ hydroxyapatite coating and crosslinking reaction of crystalline nanocellulose. *Materialia*, 4, 237-246.
- Li, M., Zhou, H., Li, T., Li, C., Xia, Z., & Duan, Y. (2015). Polyurethane/poly (vinyl alcohol) hydrogel coating improves the cytocompatibility of neural electrodes. *Neural Regeneration Research*, 10(2), 2048-2053.
- Meskinfam, M., Bertoldi, S., Albanese, N., Cerri, A., Tanzi, M., Imani, R., . . . Fare, S. (2018). Polyurethane foam/nano hydroxyapatite composite as a suitable scaffold for bone tissue regeneration.

- Materials Science and Engineering: C*, 82(1), 130-140.
- Mikulcic, H., Jin, Q., Stancin, H., Wang, X., Li, S., Tan, H., & Duic, N. (2019). Thermogravimetric analysis investigation of polyurethane plastic thermal properties under different atmospheric conditions. *Journal of Sustainable Development of Energy, Water, and Environment Systems*, 7(2), 355-367.
- Naqshbandi, A., Sopyan, I., & Gunawan. (2013). Development of porous calcium phosphate bioceramics for bone implant applications: a review. *Recent Patents on Materials Science*, 6, 238-252.
- Nunez, D., Elgueta, E., Varaprasad, K., & Oyarzun, P. (2018). Hydroxyapatite nanocrystals synthesized from calcium rich bio-wastes. *Materials Letters*, 230, 64-68.
- Trovati, G., Sanchez, E., Neto, S., Mascarenhas, Y., & Chierice, G. (2010). Characterization of polyurethane resins by FTIR, TGA, and XRD. *Journal of Applied Polymer Science*, 115, 263-268.
- Waluyo, A., & Sabarman, H. (2019). Fabrikasi fiber polyvinyl alcohol (PVA) dengan elektrospinning. *Gravity: Jurnal Ilmiah Penelitian dan Pembelajaran Fisika*, 5 (1), 88-98
- Zhang, X., Zhang, L., Li, Y., Hua, Y., Li, Y., Li, W., & Li, W. (2019). Template-assisted, Sol-gel Fabrication of Biocompatible, Hierarchically Porous Hydroxyapatite Scaffolds. *Materials*, 12, 1274.